Cell, Vol. 95, 307–318, October 30, 1998, Copyright ©1998 by Cell Press

Protein Kinase C as a Molecular Machine for Decoding Calcium and Diacylglycerol Signals

Elena Oancea and Tobias Meyer*
Department of Cell Biology
Duke University Medical Center
Durham, North Carolina 27710

Summary

The specificity of many signal transduction pathways relies on the temporal coordination of different second messenger signals. Here we found a molecular mechanism which guarantees that conventional protein kinase C (PKC) isoforms are sequentially activated by calcium and diacylglycerol signals. Receptor stimuli that triggered repetitive calcium spikes induced a parallel repetitive translocation of GFP-tagged PKCγ to the plasma membrane. While calcium acted rapidly, diacylglycerol binding to PKCγ was initially prevented by a pseudosubstrate clamp, which kept the diacylglycerol-binding site inaccessible and delayed calcium- and diacylglycerol-mediated kinase activation. After termination of calcium signals, bound diacylglycerol prolonged kinase activity. The properties of this molecular decoding machine make PKCγ responsive to persistent diacylglycerol increases combined with high- but not low-frequency calcium spikes.

Introduction

Receptor-mediated signal transduction processes utilize the same signaling proteins and second messengers to induce different cellular functions. The fundamental question then arises of how specificity can be achieved for a particular signaling pathway. This question is particularly relevant for the second messengers calcium and diacylglycerol that are generated by the activation of numerous receptor stimuli and that jointly mediate cell functions that range from gene expression, secretion, and cytoskeletal restructuring to cell migration and cell growth. Our study tests the hypothesis that the temporal coordination of calcium and diacylglycerol signals can selectively activate enzymes. Calcium signals often appear as repetitive calcium spikes (transient increases in calcium concentration) that can be induced by electrical or receptor stimuli (reviewed in Tsien and Tsien, 1990; Meyer and Stryer, 1991; Berridge, 1993; Thomas et al., 1996). Repetitive calcium spikes typically increase their frequency with the amplitude of the receptor stimuli. In marked difference, receptor-induced diacylglycerol increases are typically prolonged and often biphasic (reviewed in Quest, 1996) and have a slower rate of production (Oancea et al., 1998).

The frequency of calcium spikes or calcium oscillations can be of critical importance for the induction of selective cellular functions. Evidence for such a role of repetitive calcium spikes was found for the activation of mitochondrial ATP production (Hajnoczky et al., 1995) and gene expression (Dolmetsch et al., 1998; Li et al. 1998), as well as for the activation of CaMKII (Meyer et al., 1992; De Koninck and Schulman, 1998). Considering the important roles of repetitive calcium spikes for these processes, the calcium decoding hypothesis can be taken one step further: a synergistic activation of PKC isoforms by calcium and diacylglycerol may turn these kinases into molecular machines that decode some combinations of calcium and diacylglycerol signals while rejecting others.

PKC isoforms have been grouped into three classes (reviewed in Nishizuka, 1992, 1988). Conventional PKC isoforms or cPKC (PKCα, PKCβ, PKCβ′, and PKCγ) have been found to be activated by calcium and diacylglycerol, nPKC isoforms by diacylglycerol alone, while the activation of aPKC isoforms is only little understood. We have focused this study on PKCγ as an example for cPKC isoforms. Conventional PKC isoforms can be activated by hormonal, neurotransmitter, growth factor as well as other receptor stimuli and are involved in the regulation of other signaling pathways, gene expression, secretion, and modulation of ion channels, as well as critical roles in cell growth and differentiation (reviewed in Nishizuka, 1992). The PKCγ isoform itself is particularly important in neurons where it regulates synaptic plasticity and other neuronal functions (i.e., Abeliovich et al., 1993).

How is this important class of enzymes activated? Similar to other serine/threonine kinases, the activity of cPKC isoforms is kept low in a basal state by a pseudosubstrate sequence that is localized at the N terminus of cPKC as part of a variable region (V1-domain; Pears and Parker, 1991). Lipid vesicle binding studies have identified the nearby tandem C1- ($C1_2$-) and single C2-domains as the interaction sites for diacylglycerol and calcium, respectively. It has been proposed that activation of cPKC isoforms is the result of binding of calcium and diacylglycerol to these domains, which in turn releases the pseudosubstrate inhibitory domain (reviewed in Newton, 1995; Quest, 1996; Hurley and Gobler, 1997). Although PKC isoforms can have additional binding interactions with different cellular proteins (reviewed in Mochly-Rosen, 1995), in vitro and in vivo studies showed that calcium or phorbol esters trigger a translocation of cPKC isoforms to negatively charged vesicles (Boni and Rando, 1985), to mixed micelles (Hannun et al., 1985), or to the plasma membrane (Sakai et al., 1997, Oancea et al., 1998).

Here we explored the question of whether different combinations of calcium and diacylglycerol stimuli can selectively activate cPKC isoforms. We showed that GFP-tagged PKCγ as well as GFP-tagged minimal $C1_2$- and C2-domains all translocated to the plasma membrane in response to hormonal stimuli. The translocation of C2-GFP was regulated by calcium and the translocation of $C1_2$-GFP by diacylglycerol. For low amplitude receptor stimuli, PKCγ-GFP and C2-GFP oscillated between the plasma membrane and the cytosol in synchrony with simultaneously measured repetitive calcium

*To whom correspondence should be addressed (e-mail: tobias@cellbio.duke.edu).

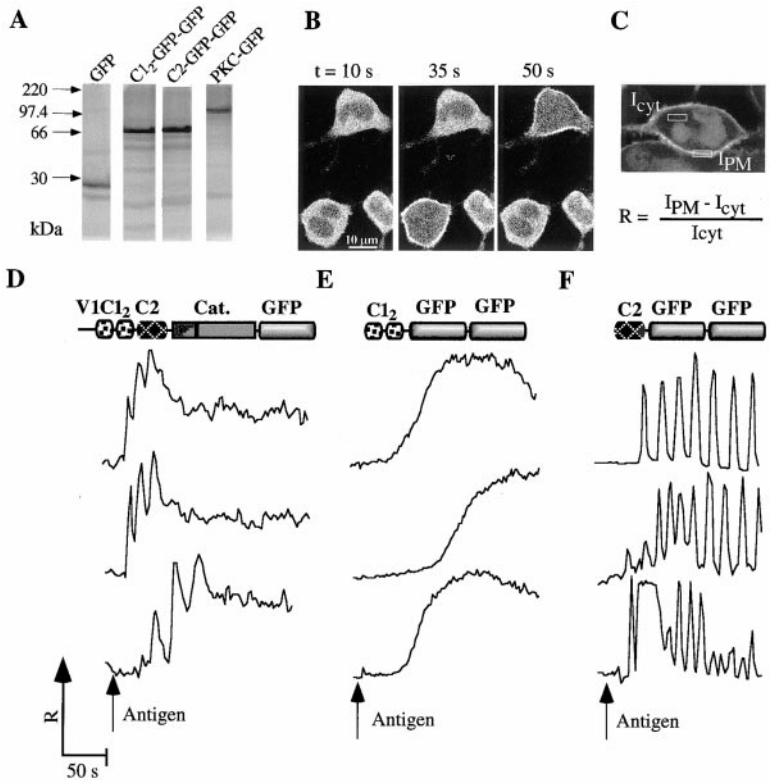

Figure 1. Receptor-Induced Translocation of PKCγ Compared to Its $C1_2$- and C2-Domain

(A) In vitro–translated PKCγ-GFP, $C1_2$-GFP, and C2-GFP constructs analyzed by SDS-PAGE.

(B) Receptor activation induces a translocation of PKCγ-GFP to the plasma membrane. The images shown were recorded 10, 35, and 50 s after addition of antigen (20 μg/ml of DNP-BSA).

(C) Definition of the relative plasma membrane translocation parameter (R).

(D) Examples of the time course of plasma membrane translocation of PKCγ-GFP. Maximal translocation of PKCγ-GFP to the plasma membrane was $R = 1.5 \pm 0.6$ ($N = 30$).

(E) Examples of the time course of plasma membrane translocation of $C1_2$-GFP. Maximal translocation was $R = 0.9 \pm 0.3$ ($N = 30$).

(F) Examples of the time course of plasma membrane translocation of C2-GFP. Maximal translocation was $R = 2.5 \pm 1.8$ ($N = 50$). The fusion constructs in (E) and (F) were tagged with tandem GFP molecules connected by a $(GA)_5$ linker sequence.

spikes. Surprisingly, while the diacylglycerol DiC8 effectively translocated $C1_2$-GFP to the plasma membrane, it had no measurable effect on full-length PKCγ-GFP. Furthermore, the phorbol ester–induced translocation of PKCγ-GFP to the plasma membrane required more than 100 s compared to a few seconds for the minimal $C1_2$-GFP alone. This marked delay and suppression in translocation suggests that the diacylglycerol-binding site is initially inaccessible in PKCγ. Deletion of the V1-domain, which contains the pseudosubstrate motif, accelerated plasma membrane translocation, showing that it is the clamping of the V1-domain to the catalytic domain that makes the diacylglycerol-binding site inaccessible. Interestingly, the V1-domain had also a plasma membrane binding capability, since PKCγ with a deleted catalytic domain was prelocalized to the plasma membrane in the absence of calcium and diacylglycerol. This suggests that diacylglycerol binding to the $C1_2$-domain requires an opening of the V1-clamp and an interaction of the V1-domain with the plasma membrane.

When PKCγ-GFP was translocated to the plasma membrane during repetitive calcium spiking, its binding to phorbol ester or diacylglycerol was still delayed, albeit the time required for binding was much shorter (10 s). Once activated by diacylglycerol, PKCγ-GFP was retained at the plasma membrane by diacylglycerol for a time period of 8 s, even after the termination of a calcium spike. While the initial delay in diacylglycerol binding provides a mechanism to suppress PKCγ activation for low-frequency calcium spikes, the retention of PKCγ-GFP at the plasma membrane after the termination of a calcium spike provides a mechanism for prolonging and integrating PKCγ activity. Thus, the activation of cPKC isoforms is defined by three key features: (1) sequential plasma membrane–binding interactions of the C2-, V1-, and $C1_2$-domains that result from the calcium binding to the C2-domain, the opening of the V1-clamp, and the diacylglycerol binding to the $C1_2$-domain; (2) a delayed activation of cPKC by diacylglycerol and calcium signals; and (3) a prolonged activity of cPKC after termination of a calcium spike. These features enable cPKC isoforms to reject calcium or diacylglycerol signals that are triggered separately and to be only minimally and reversibly activated by diacylglycerol signals combined with low-frequency and short calcium spike. In contrast, diacylglycerol signals combined with high-frequency calcium spikes can gradually increase cPKC activity to a maximal sustained level.

Results

$C1_2$- and C2-Domains of PKCγ Act as Individual Plasma Membrane–Binding Modules

We investigated the calcium- and diacylglycerol-mediated activation of PKCγ by comparing the translocation of GFP-tagged PKCγ (PKCγ-GFP) to that of its diacylglycerol-binding domain ($C1_2$-GFP) and of its calcium-binding domain (C2-GFP). The GFP constructs were cloned into a vector optimized for RNA transfection (Yokoe and Meyer, 1996), and the size of the expressed proteins was verified by in vitro translation and SDS-PAGE analysis (Figure 1A). An earlier study has shown that a C-terminal GFP tag does not affect the catalytic activity and the cofactor dependence of PKCγ (Sakai et al., 1997).

Figure 1B shows images of antigen-stimulated RBL

cells expressing PKCγ-GFP. The three images were taken 10, 35, and 50 s after stimulation and show cell specific differences in the time courses of plasma membrane translocation of PKCγ-GFP. Antigen-stimulation of IgE receptors (FcεRI) was used for phospholipase Cγ activation and the generation of calcium and diacylglycerol signals (i.e., Schneider et al., 1992). To analyze the kinetics of the translocation process, series of 100 images were taken at varying time intervals between images and the relative increase in the plasma membrane over cytosolic fluorescence intensity (R) was calculated at each time point (Figure 1C). This relative plasma membrane translocation parameter was graphed as a function of time for each cell analyzed.

Full-length PKCγ-GFP translocated to the plasma membrane with variable time courses (Figure 1D). For the maximal receptor stimuli shown in the three examples, translocation often had an initially oscillatory appearance that was then followed by a persistent plasma membrane localization. These rapid oscillatory localizations were not observed for $C1_2$-GFP (Figure 1E). Instead, $C1_2$-GFP gradually translocated to the plasma membrane over a 50–200 s long time period, suggesting that it binds to the plasma membrane in response to a slow accumulation of diacylglycerol. Strikingly, the calcium sensing C2-GFP showed an oscillatory plasma membrane translocation, reminiscent of receptor-triggered calcium spikes (Figure 1F).

Oscillations in the Translocation of PKCγ and C2-Domains Are Synchronous with Repetitive Calcium Spikes

To investigate the oscillatory translocation of the C2-GFP and PKCγ-GFP to the plasma membrane, we microporated the calcium indicator Calcium-Crimson Dextran (70 kDa) together with the RNA for either C2-GFP or PKCγ-GFP. After expression of the GFP-tagged protein, the antigen-induced change in fluorescence of the calcium indicator (excitation at 568 nm) was imaged simultaneously with the translocation of the GFP-tagged proteins (excitation at 488 nm). To reduce the production of diacylglycerol and trigger continuous repetitive calcium spikes, a low concentration of antigen was used (100 ng/ml DNP-BSA). The upper panels in Figure 2A show masked ratio-images of the calcium indicator, while the lower panels show changes in the translocation of C2-GFP at different times after stimulation. A correlation between an increase in calcium concentration and the plasma membrane translocation of C2-GFP can be observed.

Figure 2B shows typical time courses of calcium spikes versus the plasma membrane translocation of C2-GFP and PKCγ-GFP. The calcium ionophore ionomycin was added at the end of the experiment to calibrate the calcium signal and to induce maximal translocation of the GFP-constructs. The calculated peak amplitudes show that an increase in intracellular calcium of as small as 200 nM can induce a measurable translocation from cytosol to plasma membrane of either C2-GFP or PKCγ-GFP. More importantly, this analysis directly shows that intracellular calcium spikes closely correlate not only with the translocation of C2-domains, but also with the translocation of full-length PKCγ.

When the transfected cells were stimulated in the absence of extracellular calcium, the oscillations in the plasma membrane translocation of C2-GFP could still be observed, although they typically stopped after a time period of 200 s or less (Figure 2C). Thus, calcium influx from the extracellular space is not required to induce the oscillations in the translocation of the C2-domain.

The Diacylglycerol-Binding Sites of PKCγ Are Inaccessible in the Inactive Kinase

While it has been shown that cPKC isoforms require calcium as well as diacylglycerol to be fully active (Hannun et al., 1985), little is known about the activation steps that lead to maximal kinase activity. As shown in the first model in Figure 3A, PKCγ could be in an "inside/inside" configuration where neither the calcium- nor the diacylglycerol-binding sites would face the outside of the protein. This conformation would require conformational changes before diacylglycerol or calcium could bind. In a second model, the calcium- and diacylglycerol-binding sites could be in an "outside/outside" configuration in which both domains could rapidly bind their respective second messenger. The third and fourth possibilities are "inside/outside" and "outside/inside" configurations, respectively, with only the calcium or the diacylglycerol-binding sites available for immediate binding. The interaction of the second site would be initially disabled. Thus, the translocation to the plasma membrane would be mediated by a sequential activation process.

We investigated the domain accessibility by comparing the rate of calcium- or phorbol ester–induced plasma membrane translocation of $C1_2$-GFP and C2-GFP to that of PKCγ-GFP. Addition of calcium ionophore to cells expressing C2-GFP or PKCγ-GFP led to a rapid translocation of both constructs to the plasma membrane (Figure 3B). In contrast, the addition of the phorbol ester PDBu triggered a rapid translocation of $C1_2$-GFP and a markedly slower translocation of PKCγ-GFP. Figure 3C shows that PKCγ-GFP translocation is still submaximal after 100 s, while the cytosolic C1-GFP is already maximally translocated. A quantitative analysis of the translocation kinetics is shown in Figures 3D to 3F. C2-GFP and PKCγ-GFP translocated to the plasma membrane in less than 10 s after addition of calcium ionophore, suggesting that the calcium-binding site in the C2-domain is readily accessible in an "outside" configuration. The rapid translocation of PKCγ-GFP in response to calcium signals is in marked contrast to its slow translocation in response to addition of PDBu. While $C1_2$-GFP translocated to the plasma membrane in a few seconds after PDBu addition, translocation of PKCγ-GFP took more than 100 s to be half completed (Figure 3E). This suggests that the diacylglycerol-binding sites in the $C1_2$-domain are in an "inside" configuration and are not readily accessible to interact with PDBu. In control experiments, the joint addition of calcium ionophore and PDBu translocated all three constructs rapidly to the plasma membrane (Figure 3F).

We also tested the effect of the membrane permeant diacylglycerol DiC8 on the kinetics of translocation. Interestingly, DiC8 induced only translocation of $C1_2$-GFP

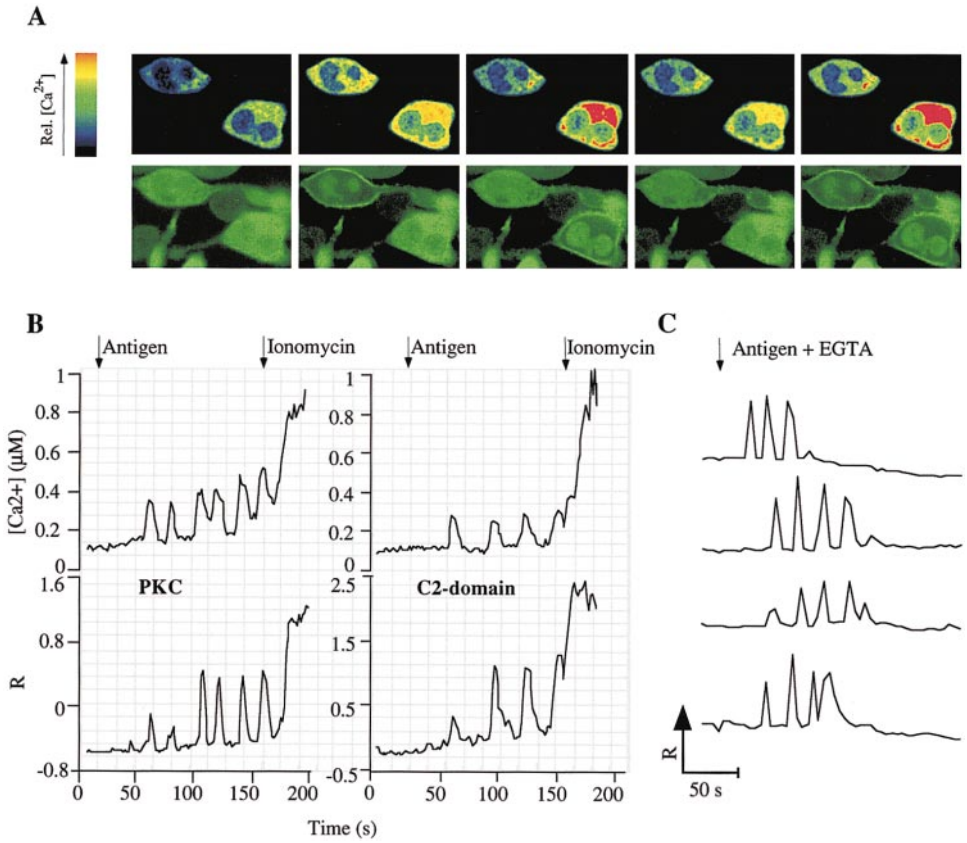

Figure 2. Oscillations in the Translocation of PKCγ and the C2-Domain Are Synchronous with Repetitive Calcium Spikes

(A) Parallel measurements of calcium signals and C2-GFP plasma membrane translocation. Cells were comicroporated with Calcium-Crimson dextran (70 kDa) and C2-GFP RNA. After three or more hours of expression, cells were stimulated with 2 μg/ml DNP-BSA, and the changes in fluorescence intensity were simultaneously imaged for the calcium indicator and the C2-GFP probe. The five images shown were taken 24, 104, 114, 130, and 139 s after stimulation. Color-coded ratio images are shown for the calcium responses.

(B) Time course of calcium signals compared to the plasma membrane translocation of C2-GFP (left) and PKCγ-GFP (right). Antigen was added at t = 15 s, followed by the calcium ionophore ionomycin at t = 160 s to determine an apparent free calcium concentration. The time course of calcium signals and the translocation of either C2-domains or PKCγ showed a marked correlation.

(C) Repetitive C2-domain translocation persisted in the absence of extracellular calcium for approximately 2 min. EGTA (5 mM) was added together with the antigen to lower extracellular calcium concentration.

without showing a measurable effect on PKCγ-GFP (Figure 3G). This lack of translocation is probably due to a lower affinity of PKC for diacylglycerol than for phorbol ester (i.e., Mosior and Newton, 1996) and to the inaccessibility of the diacylglycerol-binding sites in the inactive protein. Together, these kinetic measurements are consistent with the interpretation that the diacylglycerol-binding sites in the $C1_2$-domain in PKCγ are in an inside conformation, while the calcium-binding site in the C2-domain is in an outside orientation ("inside/outside" model in Figure 3A).

The Pseudosubstrate V1-Domain Clamps the Diacylglycerol-Binding Sites in an Inside Orientation

Previous studies have shown that the variable domain (V1) at the N terminus of cPKC contains a basic RKGA LRQ motif that serves as a pseudosubstrate or autoinhibitory sequence that binds to the catalytic domain and keeps the kinase in an inactive state (Pears and Parker, 1991). In this widely accepted model, activation of PKC occurs by releasing the bound pseudosubstrate domain from the catalytic domain. Taken together with the data in Figure 3, it is then suggestive to propose that the pseudosubstrate domain not only keeps the protein in the inactive state, but also clamps the $C1_2$-domain in its inside orientation.

To test this hypothesis, we removed the V1-domain of PKCγ and compared the PDBu-induced time course of translocation of PKCγ-GFP to that of the deletion mutant, PKCγ(ΔV1)-GFP (Figure 4A). Consistent with the hypothesis, the time required for plasma membrane translocation of PKCγ(ΔV1)-GFP was much more rapid than that of PKCγ-GFP. Indeed, the rate of translocation of PKCγ(ΔV1)-GFP was indistinguishable to that of $C1_2$-GFP. As a control, Figure 4B shows that the removal of the V1-domain had no effect on the ionomycin-induced translocation.

In order to test whether the mechanism that restricts the orientation of the C1-domain is indeed a binding

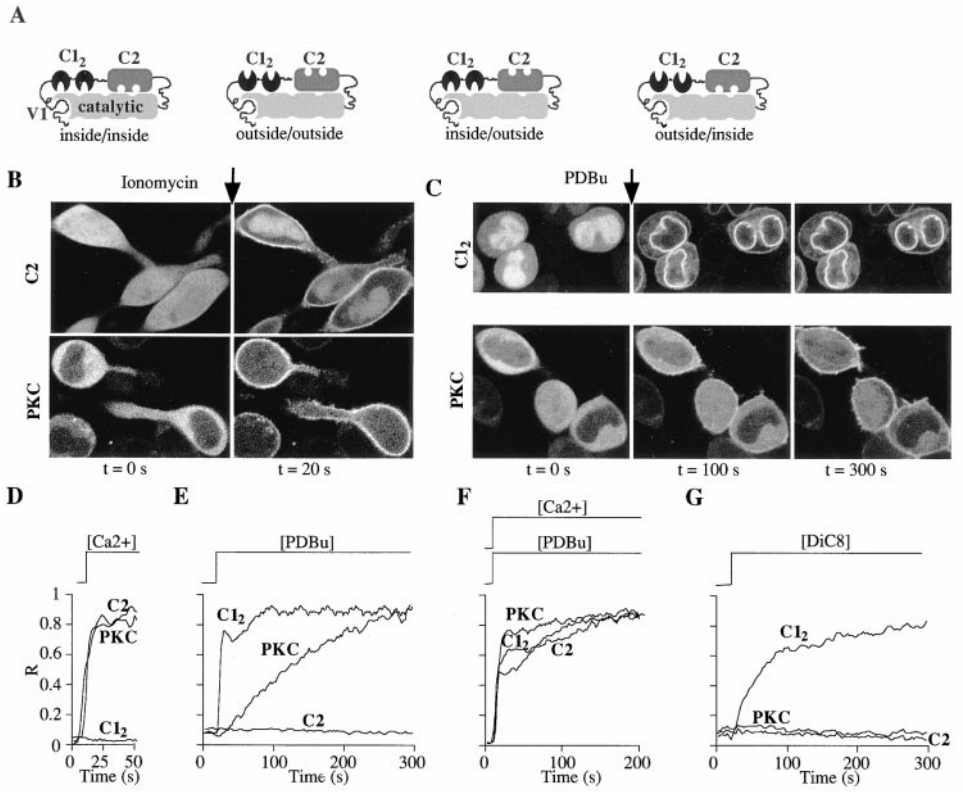

Figure 3. The Diacylglycerol-Binding Site Is Inaccessible in Inactive PKCγ

(A) Potential models for the initial orientations of the diacylglycerol-binding sites in the $C1_2$-domain and the calcium-binding site in the C2-domain. The $C1_2$- and C2-domains are shown in "inside-inside," "outside-outside," "inside-outside", or "outside-inside" orientations, respectively.

(B) Confocal fluorescence images of RBL cells expressing C2-GFP (upper panel) or PKCγ-GFP (lower panel). When ionomycin (1 μM) was added to cells expressing either C2-GFP or PKCγ-GFP, maximal translocation of PKCγ-GFP as well as C2-GFP occurred rapidly. Twenty second time points are shown in the right panels.

(C) When PDBu (1 μM) was added to cells expressing either $C1_2$-GFP (upper panel) or PKCγ-GFP (lower panel), a translocation of the two GFP fusion proteins occurred with markedly different time courses. The middle panels, taken 100 s after stimulation, show that $C1_2$-GFP is maximally translocated while PKCγ-GFP is only partially translocated. PKCγ-GFP reaches maximal translocation only after 300 s (lower right panel). It should be noted that a significant fraction of $C1_2$-GFP is nuclear localized in the unstimulated cell and rapidly translocated to the nuclear membrane after PDBu addition.

(D) Time course of the plasma membrane translocation of $C1_2$-GFP, C2-GFP, and PKCγ-GFP after addition of the calcium ionophore ionomycin. The relative plasma membrane translocation in a series of sequential images was calculated as shown in Figure 1D. The rapid translocation time course observed for the C2-GFP and the PKCγ-GFP suggests an "outside" orientation for the calcium-binding sites of the C2-domain in PKCγ.

(E) Time course of the plasma membrane translocation of $C1_2$-GFP, C2-GFP, and PKCγ-GFP after addition of the phorbol ester PDBu. The rapid translocation time course observed for $C1_2$-GFP is contrasted by a much slower time course of PKCγ-GFP translocation, suggesting an "inside" orientation of the diacylglycerol-binding sites of the $C1_2$-domain in PKCγ.

(F) Control measurements showing the rapid time course of the plasma membrane translocation of all constructs after simultaneous addition of PDBu and ionomycin.

(G) Time course of the plasma membrane translocation of $C1_2$-GFP, C2-GFP, and PKCγ-GFP after addition of the plasma membrane permeant diacylglycerol DiC8. DiC8 induces only a plasma membrane translocation of $C1_2$-GFP and has no measurable effect on PKCγ-GFP translocation. Each trace shown on the graphs in (C) to (G) represents an average of 12–18 cells obtained from at least three different experiments.

interaction between the V1-domain and the catalytic domain of PKCγ, we compared the time course for translocation of the two constructs used above but lacking the catalytic domain, $C1_2$-C2-GFP and V1-$C1_2$-C2-GFP. Figure 4C shows that both constructs rapidly translocate to the plasma membrane after PDBu addition with a near identical time course of translocation. This further supports the hypothesis that the accessibility of the C1-domain is controlled by a "clamp" between the V1-domain and the catalytic domain. To clarify this conclusion, the predicted configuration of the diacylglycerol- and calcium-binding sites are shown in two schemes in Figure 4D for PKCγ with and without the pseudosubstrate V1-clamp.

The V1-Domain Can Switch between a Strong Binding with the Catalytic Domain and a Weak Binding with the Plasma Membrane

To investigate the role of the V1-domain in the PKCγ activation process, we determined whether an interaction between the V1-domain and negatively charged

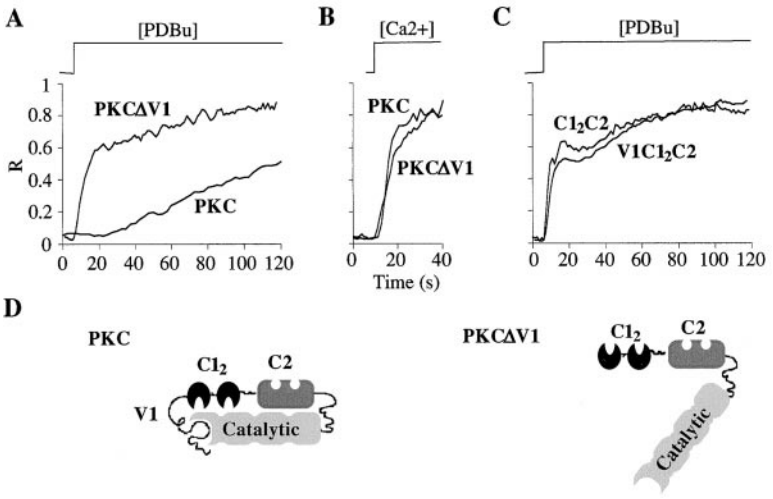

Figure 4. The V1-Domain Functions as a Clamp that Binds to the Catalytic Domain and Prevents Diacylglycerol Binding

(A) Comparison of the time course of PDBu-induced plasma membrane translocation of full-length PKCγ-GFP and a deletion mutant that lacks the V1-domain PKCγ(ΔV1)-GFP. The relative plasma membrane translocation (R) is represented as a function of time. The time required for full-length PKCγ-GFP translocation is much shorter than the time required for PKCγ(ΔV1)-GFP translocation. This is consistent with the hypothesis that the V1-domain serves as a clamp that makes the $C1_2$-domain inaccessible for diacylglycerol and phorbol ester.

(B) Control measurement, showing that ionomycin (1 μM) induces a similar time course of translocation for PKCγ-GFP and PKCγ(ΔV1)-GFP, suggesting that the removal of the V1-domain does not affect the calcium-binding properties of the C2-domain.

(C) Comparison of the time course of PDBu-induced plasma membrane translocation of the same constructs as in (A) but without the catalytic domain ($C1_2$-C2-GFP and V1-$C1_2$-C2-GFP). The time required for V1-$C1_2$-C2-GFP translocation was indistinguishable from the time required for $C1_2$-C2-GFP translocation. This is consistent with the hypothesis that the $C1_2$-domain is kept inaccessible by a clamp between the V1-domain and the catalytic domain. Each of the traces shown in (A), (B), and (C) represent an average of 12–15 cells from at least three different experiments.

(D) Schematic representation of the structural arrangement of the PKCγ construct (left) and the PKCγ(ΔV1) construct (right).

vesicles that was observed in vitro (Mosior and McLaughlin, 1991) may reflect a membrane binding interaction in the cellular environment. Indeed, while $C1_2$-C2-GFP had a homogeneous distribution (Figure 5A, left panel), V1-$C1_2$-C2-GFP was partially prelocalized to the plasma membrane in the unstimulated state (Figure 5B, left panel). As expected, a rapid and maximal translocation of both constructs could be induced by addition of calcium ionophore (Figures 5A and 5B, right panels). The partial prelocalization of V1-$C1_2$-C2-GFP to the plasma membrane strongly suggests that the V1-domain has the capability to selectively bind to the plasma membrane if it is not bound to the catalytic domain.

Since no plasma membrane prelocalization was observed for PKCγ-GFP in the absence of calcium and diacylglycerol signals (see Figure 1B), it is likely that the interaction of the V1-domain with the catalytic domain is much stronger than its interaction with the plasma membrane. Furthermore, the only partial prelocalization of V1-$C1_2$-C2-GFP to the plasma membrane suggests that the binding interaction of the V1-domain with the plasma membrane is relatively weak. This was confirmed by fluorescence recovery after photobleaching measurements in which a small region of the plasma membrane was photobleached and the gradual recovery of the fluorescence intensity of the bleached region was recorded as a function of time (Figure 5C). As expected for a weak binding interaction, we observed a markedly faster recovery of V1-$C1_2$-C2-GFP in the absence of stimuli when compared to the recovery time course after addition of either ionomycin or DiC8 (Figure 5D). These recovery time courses for V1-$C1_2$-C2-GFP in the presence of ionomycin and DiC8 were also indistinguishable from those of $C1_2$-C2-GFP (data not shown).

In order to obtain apparent diffusion coefficients and dissociation time constants for the plasma membrane bound V1-$C1_2$-C2-GFP, the profiles of the photobleached region were fit as a function of time using Gaussian functions (Oancea et al., 1998). The apparent dissociation time constant and diffusion coefficient were $D = 0.236 \pm 0.060\ \mu m^2/s$ and $\tau = 282 \pm 76$ s in the presence of ionomycin compared to $D = 0.080 \pm 0.013\ \mu m^2/s$ and $\tau = 421 \pm 77$ s in the presence of DiC8. In the absence of ionomycin or DiC8, the only partially plasma membrane localized V1-$C1_2$-C2-GFP could not be analyzed by this method since the fraction of residual cytosolic protein was too high. Nevertheless, this analysis supports the hypothesis that the binding interaction of the V1-domain with the plasma membrane is significantly weaker than the one mediated by the C2-domain, which in turn is weaker than the interaction mediated by the $C1_2$-domain.

Calcium Signals Accelerate PDBu Binding to PKCγ

Together, the above described results suggest that PKCγ activation is a result of sequential plasma membrane–binding interactions of C2-, V1-, and $C1_2$-domains. Can such a sequential activation model be directly tested? In our working hypothesis, calcium signals would translocate PKCγ to the plasma membrane and serve as a "priming factor" for enzyme activation. The V1-domain would then act as a switch that regulates the accessibility of the $C1_2$-domain. This model would then predict that an increase in calcium concentration should significantly accelerate the more than 100 s delay in the binding interaction of PDBu with PKCγ at basal calcium concentration.

To test the prediction of our working model, we analyzed the binding interaction of PDBu with PKCγ-GFP during calcium spiking. For comparison, Figure 6A shows the antigen-induced repetitive translocation of PKCγ-GFP and Figure 6B shows the PDBu-induced slow translocation of PKCγ-GFP. Three typical single cell traces are shown for both stimuli. In contrast, PDBu addition to cells prestimulated with antigen had a markedly different result (Figure 6C) that could not be explained by a superposition of the translocation events

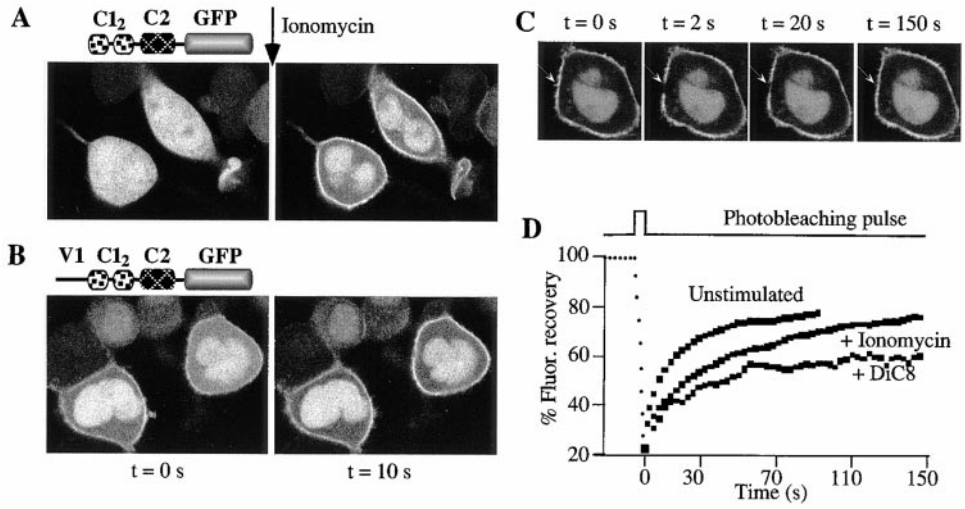

Figure 5. The V1-Switch: V1-Domain Binding to the Plasma Membrane

(A) $C1_2$-C2-GFP is cytosolic in unstimulated cells and rapidly translocates to the plasma membrane after addition of ionomycin. Two images of an RBL cell before and 10 s after ionomycin addition are shown.

(B) V1-$C1_2$-C2-GFP is partially prelocalized to the plasma membrane in unstimulated RBL cells, suggesting that V1-domains can mediate an additional plasma membrane–binding interaction. Maximal plasma membrane localization can be induced by addition of ionomycin. Two images of an RBL cell before and 10 s after ionomycin addition are shown.

(C) Fluorescence recovery after photobleaching was used as a method to compare the binding of the V1-, $C1_2$-, or C2-domain with the plasma membrane. After photobleaching a small region of the plasma membrane, the fluorescence of the photobleached region was monitored in a series of 50 images, 3 s apart. The images shown represent RBL cells expressing V1-$C1_2$-C2-GFP recorded before and 2, 20, and 150 s after photobleaching. The arrow points to the photobleached area.

(D) Fluorescence recovery is shown as a function of time for V1-$C1_2$-C2-GFP. In the unstimulated state, the V1-domain mediates a partial plasma membrane prelocalization that shows rapid recovery. The recovery time course in the presence of ionomycin is markedly slower and is even more reduced in the presence of DiC8.

in Figures 6A and 6B: PDBu rapidly stabilized PKCγ-GFP at the plasma membrane after its translocation by a calcium spike. The first two cells in Figure 6C show examples of a stabilization of PKCγ-GFP at its peak amplitude, while the third example shows a cell where the stabilization occurs halfway during the termination of a calcium spike. In all cells, PDBu induced a rapid stabilization at the plasma membrane only when PKCγ-GFP was "primed" by a calcium spike.

Since physiological calcium spikes are often very short, it is important to determine how long a calcium spike has to last to allow translocated PKCγ to interact with diacylglycerol or PDBu that is already present in the plasma membrane. The time required for the binding of PDBu was measured by fluorescence photobleaching recovery. Using photobleaching recovery, we observed a marked difference in the initial rate of fluorescence recovery for PKCγ-GFP targeted to the plasma membrane by calcium alone (1.35%/s) and by a combination of calcium and PDBu (0.4 %/s) (Figure 6D). These rates were measured from five images during the first 4.8 s after the photobleaching pulse. To measure the delay time for PDBu binding, we determined these initial rates of fluorescence recovery at different time intervals after PDBu addition.

Interestingly, the time required for a half-maximal reduction in the initial fluorescence recovery rate was 10 ± 2 s (Figure 6E), showing that calcium signals reduce the interaction time of PDBu with the $C1_2$-domain from approximately 100 s to 10 s. This result is consistent with the measurement in Figure 6C that showed that PDBu binding can be markedly accelerated by calcium-mediated translocation of PKCγ. However, although the calcium binding to the plasma membrane accelerated PDBu binding, the remaining delay of 10 s can serve as a potent mechanism to suppress PKCγ activation in response to short calcium signals.

Since our results in Figure 3G showed that diacylglycerol alone does not mediate a significant translocation of PKCγ, it becomes important to know for how long diacylglycerol can keep PKCγ active at the plasma membrane after termination of a calcium transient. Such a delay in the dissociation could act as a "memory" process that would allow PKCγ to integrate the activation signals during high-frequency repetitive calcium spiking.

Diacylglycerol Prolongs the Transient Translocation of PKCγ during Calcium Spiking

We compared the time required for PKCγ-GFP to dissociate from the plasma membrane after termination of a calcium spike in the absence and presence of the externally added diacylglycerol DiC8. Low concentrations of antigen were used in these studies in order to generate repetitive calcium spikes while only generating low concentrations of cellular diacylglycerol. As shown in Figure 7A, PKCγ-GFP rapidly dissociated from the plasma membrane with the termination of each calcium spike. In contrast, when DiC8 was added to cells during repetitive calcium spiking, the dissociation of PKCγ-GFP was markedly delayed after each spike (Figure 7B). For low antigen concentrations and in the absence of externally added DiC8, the half-maximal dissociation

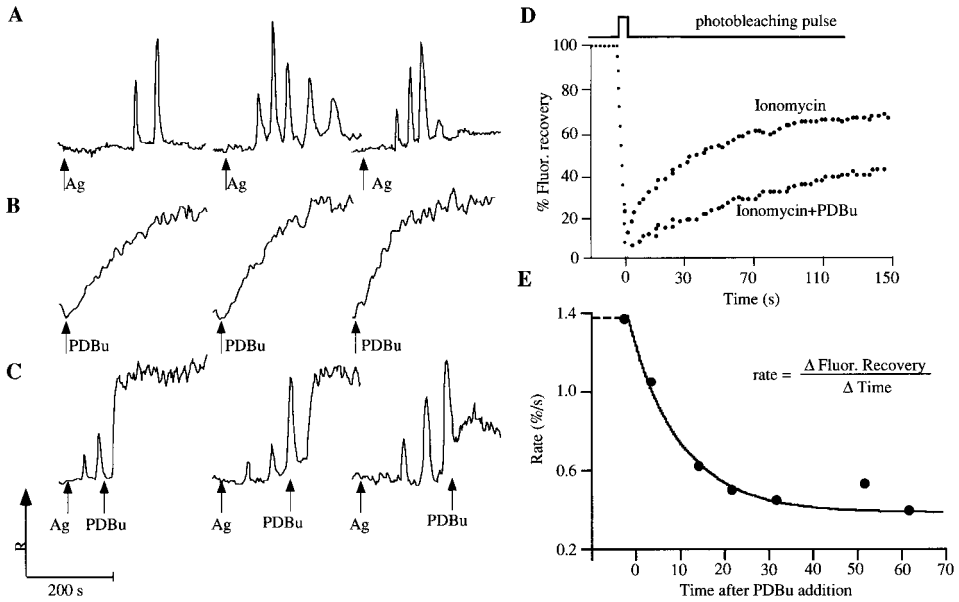

Figure 6. Delayed PDBu-Induced Activation of PKCγ

(A) For comparison, three typical examples are shown of the antigen-induced repetitive translocation of PKCγ-GFP to the plasma membrane. DNP-BSA (100 ng/ml) was used for stimulation. Each trace shows the relative change in the plasma membrane intensity (R) in a single cell as a function of time.

(B) For comparison, three typical examples are shown of the PDBu induced much slower translocation of PKCγ to the plasma membrane.

(C) PDBu rapidly stabilized PKCγ-GFP at the plasma membrane when translocated by a calcium spike. The addition of PDBu to antigen-stimulated cells shows a translocation time course that cannot be explained by the superposition of (A) and (B).

(D) Measurement of the initial rate of photobleaching recovery of PKCγ-GFP. The initial rates were calculated for the recovery slope from first five images (in a 4.8 s interval). Initial rates for recovery were 1.35%/s in the presence of ionomycin alone and were 0.4%/s in the presence of ionomycin plus PDBu.

(E) Time course of the change in the initial rate of recovery as a function of time after PDBu addition. For each time point, the photobleaching pulse was applied at different times after PDBu addition. The delay time shown on the x axis represents the elapsed time between PDBu addition and the photobleaching recovery protocol, corrected for a 6 s delay for PDBu to diffuse through the membrane and a 2.4 s interval to the middle image used for the slope analysis. A 10 ± 2 s long delay between the increase in PDBu concentration and the tightening in binding affinity of PKCγ-GFP was measured.

typically preceded the half-maximal drop in calcium concentration, presumably due to a cooperative calcium dependence of the C2-domain binding to the plasma membrane.

The average delays in the presence and absence of DiC8 were analyzed by comparing the half-maximal plasma membrane dissociation of PKCγ-GFP to the half-maximal drop in cytosolic calcium concentration (Figure 7C). Figure 7D shows that the average delay between the half-maximal drop in calcium concentration and the half-maximal membrane dissociation of PKCγ-GFP was $\Delta t = -1.2$ s in the absence of DiC8 and $\Delta t =$ 8 s in the presence of DiC8. This suggests that an important function of diacylglycerol is to prolong PKCγ activity by delaying the plasma membrane dissociation after a calcium spike.

Discussion

GFP-Tagged C2-, C1-, and Other Minimal Protein Domains as Fluorescent Translocation Indicators

Our study provides an interesting case study for using GFP-tagged minimal protein domains as fluorescent translocation indicators to monitor particular signal transduction processes in living cells. Since the translocation of minimal GFP-tagged C2- and C1-domains likely occurs for calcium and diacylglycerol signals in all cell types, these probes can be used as selective indicators for either calcium or diacylglycerol signals. As an example of the ability to dynamically monitor calcium signals with C2-GFP, a movie of the receptor-induced repetitive translocation of C2-GFP is shown at http://www.cell.com/cgi/content/full/95/3/307/DC1.

What are the advantages of fluorescent translocation indicators? Recent studies have shown that tyrosine phosphorylation and different types of lipid second messengers can be studied with such minimal signaling domains (Stauffer and Meyer, 1997; Kontos et al., 1998; Oancea et al., 1998; Stauffer et al., 1998). Fluorescent translocation indicators typically have a high signal over background and are in many cases better suited for studying signal transduction mechanisms than the alternative approach of using constructs with pairs of GFP color variants that exhibit a signal-induced change in fluorescent energy transfer (Miyawaki et al., 1997; Romoser et al., 1997). Practical experience has shown that it is often difficult to generate constructs that will show a sufficiently large change in fluorescence energy transfer for a particular signaling protein or signaling domain. Thus, fluorescent translocation indicators can provide

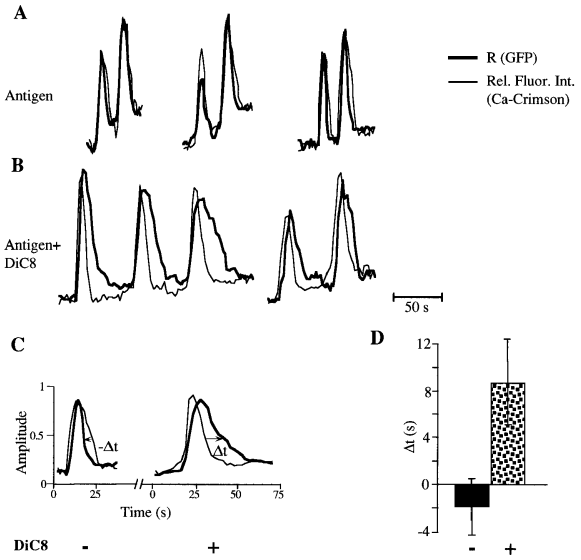

Figure 7. External Addition of DiC8 Delays the Dissociation of PKCγ from the Plasma during Calcium Spiking

(A) Overlay of the fluorescence intensity of Calcium-Crimson dextran (thin line) and the plasma membrane translocation of PKCγ-GFP (thick line) recorded from antigen-stimulated RBL cells (100 ng/ml of DNP-BSA). The half-maximal dissociation of PKCγ-GFP from the plasma membrane occurred slightly before the half-maximal decrease in relative calcium concentration. Responses of three representative cells are shown.

(B) Overlay of the fluorescence intensity of Calcium-Crimson dextran (thin line) and the plasma membrane translocation of PKCγ-GFP (thick line) recorded from antigen-stimulated RBL cells in the presence of 400 μg/ml DiC8. The half-maximal dissociation of PKCγ-GFP from the plasma membrane occurred significantly after the half-maximal decrease in relative calcium concentration. Responses of two representative cells are shown.

(C) Quantitative analysis of the delay between the calcium signal (thin line) and the plasma membrane translocation of the PKCγ-GFP (thick line). The time difference between the half-maximal drop in calcium concentration and the half-maximal plasma membrane dissociation of PKCγ-GFP was analyzed for each calcium spike. Typical examples of a spike in the absence (left) and presence of 400 μg/ml of DiC8 (right) are shown. In the left case were the plasma membrane dissociation of PKCγ-GFP preceded the calcium signal, the delay time Δt was considered negative.

(D) Bar diagram of the delay between the half-maximal plasma membrane dissociation of PKCγ-GFP and the half-maximal drop in calcium concentration in the presence and absence of DiC8 (N = 24).

a new class of versatile probes for signal transduction studies as well as for drug screening applications. Since both GFP-based translocation and energy transfer indicators can readily be expressed not only in cultured cells but also in transgenic animals, these probes will become particularly useful for understanding signal transduction processes in their physiological context.

The Calcium/Diacylglycerol Cycle for PKC Activation: Sequential Roles for Two Second Messengers

Our study uncovered three marked features of PKCγ that allow the kinase to be sequentially activated by calcium and diacylglycerol signals (Figure 8A). First, we showed that the pseudosubstrate V1-clamp keeps the diacylglycerol-binding $C1_2$-domain internalized and inaccessible to diacylglycerol. At the same time, the calcium-binding C2-domain can rapidly interact with the plasma membrane at elevated calcium concentration. Second, our study shows that a delayed diacylglycerol binding to the $C1_2$-domain in the presence of calcium is made possible by a reversible switch mechanism that allows the V1-domain to flicker between a strong binding with the catalytic domain and a weak binding with the plasma membrane. Third, we showed that the subsequent diacylglycerol binding to the $C1_2$-domain stabilizes the plasma membrane binding of PKCγ-GFP. In this active state, the dissociation of PKCγ-GFP from the plasma membrane is delayed after a drop in calcium concentration, suggesting that kinase activity can be prolonged by diacylglycerol after termination of a calcium spike. These findings are consistent with previous studies on the role of subdomains of cPKC isoforms that demonstrated that the $C1_2$-domain can bind two diacylglycerol molecules and that the C2-domain can bind phospholipids when complexed with two calcium ions (reviewed in Newton, 1995). Earlier studies have also identified the pseudosubstrate motif in the V1-domain of cPKC (Srinivasan et al., 1996) and showed a binding interaction of the polybasic V1-domain with anionic lipid vesicles (Mosior and McLaughlin, 1991).

Given the different time courses of calcium and diacylglycerol signals in many physiologically relevant situations, our results suggest that a reversible calcium-mediated translocation of cPKC in the absence of diacylglycerol (Figure 8B, left) has to be distinguished from a complete calcium-induced translocation and activation cycle of cPKC in the presence of diacylglycerol (Figure 8B, right). In the absence of diacylglycerol, our model predicts that calcium signals induce a rapid and reversible translocation of cytosolic cPKC to the plasma membrane [PKC(C2)-PM]. A flicker opening of the pseudosubstrate V1-domain can then become stabilized for a finite period of time by a weak binding interaction of the V1-domain with the plasma membrane [*PKC(C2/V1)-PM]. This flicker state was suggested from the observed V1-$C1_2$-C2-GFP prelocalization in Figure 5A. The release of the V1-domain interaction from the catalytic domain suggests that this is an active state of the enzyme. Therefore, the flicker state can explain the small activation of cPKC isoforms by calcium, which has been observed experimentally (Hannun et al., 1985; Sakai et al., 1997).

In the presence of diacylglycerol, our model predicts that calcium spike–mediated translocation and activation of cPKC occurs in a defined cycle in which the C2-, V1-, and $C1_2$-domains interact sequentially with the plasma membrane. The first two steps in this cycle are identical to those in the absence of diacylglycerol. As long as calcium signals are significantly shorter than 10 s, the calcium-mediated binding of cPKC to the plasma membrane [PKC(C2)-PM] is immediately reversible. The role of the flicker state [*PKC(C2/V1)-PM] is to reduce the time required for the diacylglycerol-binding interaction with the $C1_2$-domain from 200 s to 10 s by allowing cPKC to more effectively screen the plasma membrane for the presence of diacylglycerol (Figure 3). In the third step of the cycle, the delayed binding of the $C1_2$-domain to diacylglycerol stabilizes the V1-interaction with the plasma membrane and mediates maximal

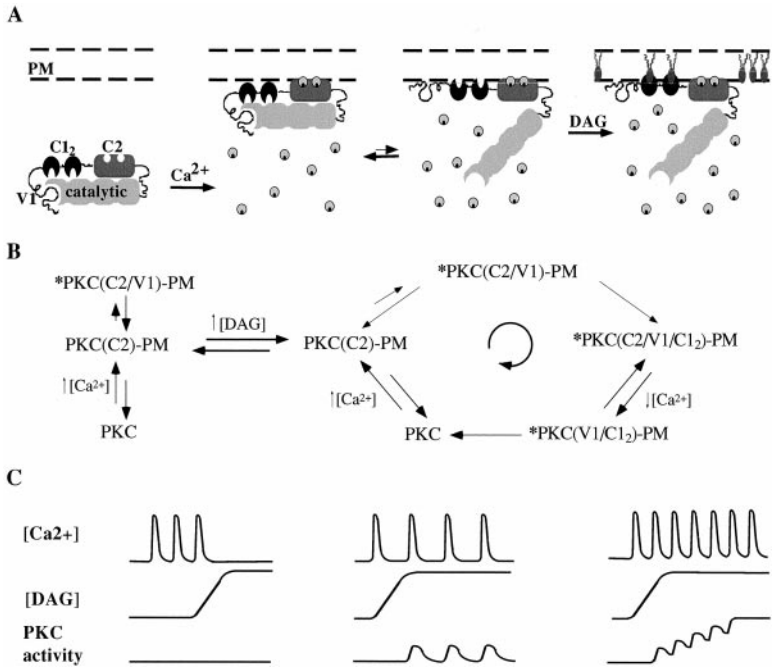

Figure 8. PKC as a Molecular Decoding Machine for Calcium and Diacylglycerol Signals

(A) Predicted structural features of PKCγ isoforms that ensure a sequential translocation and activation process.

(B) Schematic activation model, showing the cycle of cPKC activation by calcium spikes in the absence and presence of diacylglycerol. In the presence of diacylglycerol, each calcium spike induces a unidirectional activation cycle for cPKC. The steps from PKC-C2-PM to *PKC(C2/V1/$C1_2$)-PM and from *PKC(V1/$C1_2$)-PM back to cytosolic PKC introduce two critical delays in the cycle.

(C) Model for the decoding of calcium and diacylglycerol signals by cPKC isoforms. Many receptor stimuli induce calcium signals prior to a more persistent increase in diacylglycerol concentration. These calcium signals have only a minimal effect on cPKC activity (left panel). Due to the delay in $C1_2$-domain interaction, low-frequency and short calcium spikes induce a small and reversible kinase activation in the presence of diacylglycerol (middle panel). In contrast, high-frequency calcium spikes are integrated due to the delayed dissociation of cPKC and mediate maximal activation of the kinase (right panel).

kinase activation [*PKC(C2/V1/$C1_2$)-PM]. The binding of diacylglycerol to the $C1_2$-domain serves two purposes: it increases the binding affinity of cPKC with the plasma membrane, and it prevents the pseudosubstrate V1-domain from binding back to the catalytic domain. This active state then persists as long as calcium and diacylglycerol are elevated. Since we found that diacylglycerol alone is not sufficient to retain PKCγ at the plasma membrane, a drop in calcium concentration will lead to the dissociation of the kinase. However, this fourth step of the cycle is delayed by approximately 8 s (Figure 7), resulting in a transient cPKC state that can prolong kinase activity even after a drop in calcium concentration [*PKC(V1/$C1_2$)-PM]. This state is also likely active, since the binding of the higher affinity phorbol ester to the $C1_2$-domain is sufficient for maximal kinase activation independent of calcium. After its dissociation from the plasma membrane, the next cycle of translocation and activation can be started by the subsequent calcium transient. The sequential nature of this process defines cPKC isoforms as signaling machines that are driven by a unique cycle of calcium-induced translocation and diacylglycerol-mediated kinase activation.

PKC as a Molecular Decoding Machine for Calcium and Diacylglycerol Signals

As mentioned in the introduction, receptor-induced diacylglycerol signals are typically delayed but remain elevated for minutes with typically a transient and often biphasic appearance. In contrast, calcium signals are typically induced more rapidly and occur as repetitive spikes or sinusoidal oscillations with frequencies that increase with the amplitude of the receptor stimuli. This suggests that the initial calcium spike can only minimally activate cPKC (Figure 8C, left panel). Once diacylglycerol concentration is high, low-frequency calcium spikes lead to a small and oscillating cPKC activity with an activity that is reversed after each calcium spike (Figure 8C, middle panel). This submaximal activity is induced in PKCγ for calcium spikes that are much shorter than approximately 10 s, the delay time for diacylglycerol binding to the $C1_2$-domain. In contrast, high-frequency calcium spikes or persistent calcium increases can lead to an integration of cPKC activity, inducing a much higher amplitude of kinase activity as can be reached during low-frequency calcium spikes (Figure 8C, right panel). For PKCγ, which is an important mediator of neuronal plasticity, the suppression of low-frequency calcium spikes and integration of high-frequency calcium spikes could be an important mechanism in making the activation of PKCγ dependent on the pattern of electrical activity.

In conclusion, the frequency of calcium spikes, as well as the temporal coordination between calcium spikes and diacylglycerol signals, can tightly control the extent and timing of cPKC activation. Maximal and persistent activation can only be reached if high-frequency calcium spikes or persistent calcium increases and high concentrations of diacylglycerol are present at the same time. This decoding mechanism may explain how cPKC isoforms can selectively control different cellular processes by relying on selective patterns of calcium and diacylglycerol signals.

Experimental Procedures

Cloning of GFP Fusion Constructs, Cell Culturing, and RNA Transfection

The GFP tag used in this study was a variant cycle 3-GFP (Yokoe and Meyer, 1996). The PKCγ full-length sequence as well as those of subregions were amplified by PCR. The resulting PCR products were cloned at the N terminus of GFP. For individual domains and domain combinations, a double GFP tag was used in order to increase the molecular size.

For RNA transfection using the microporation method, in vitro

transcription of the different RNA constructs and electroporation was performed according to the procedure described in Yokoe and Meyer, 1996, and Teruel and Meyer, 1997. The concentration of PKCγ-GFP expressed in cells was typically between 1.2 and 2.0 μM, assuming published extinction coefficients and quantum efficiencies. Dilutions of known concentrations of fluorescein-dextran solutions between two coverslips were used for the calibration.

Rat basophilic leukemia 2H3 cells (a tumor mast cell line) were grown as described (Oancea et al., 1998). Addition of drugs to the cells was performed by dissolving PMA, PDBu, or DiC8 in DMSO and diluting them to the final concentration using extracellular buffer shortly before the experiment.

Confocal Microscopy and Photobleaching

Fluorescence confocal microscopy was used to monitor the translocation of GFP fusion constructs in response to different stimuli (Zeiss LSM410). The cells expressing GFP fusion proteins were imaged using a 488 nm laser line for excitation and either 515 nm long pass or 515–540 nm band pass filters for emission. For the calcium indicator, Ca-Crimson Dextran (70 kDa), the 568 nm line was used for excitation and a 590 nm long pass filter for emission. Midsections of the cells are shown in all images. Time series of images were recorded before and after stimulation of cells and the bleach rate for each series of images was calculated and used to correct the fluorescent intensities of images.

For the photobleaching experiments, the 488 nm line of the laser was used at maximal intensity to scan a 12 × 12 (or 30 × 30) pixel subregion of the plasma membrane, for 2 (or 4) s. To monitor the recovery of the photobleached spot, time series of 50 images, taken every 1.2 or 2.5 s were recorded after the photobleaching protocol.

Image Analysis

Time series of 50–100 confocal images were recorded for each experiment, each series containing images recorded at time intervals between 1.2 and 3 s. The time series were then analyzed using NIH Image software. For each cell expressing a GFP construct, a small region of the plasma membrane was marked by a rectangular box and the average fluorescence intensity of the region was measured for each image in the time series. For the same cell, a similar box was used to measure the fluorescence of the cytosol for each frame. For each time point, the ratio R = (plasma membrane fluorescence − cytosolic fluorescence)/(cytosolic fluorescence) was calculated as representing the relative increase in the plasma membrane fluorescence intensity over the cytosol, for the particular cell measured. These values were then plotted as a function of time and then normalized. The graphs were obtained by averaging traces from different experiments.

When the red calcium indicator Calcium-Crimson Dextran was used, the fluorescence intensity was measured in the cytosolic region of each cell for each image of the time series and then plotted as a function of time. The ratio images were obtained by masking the original images and dividing them by a reference image. To emphasize the changes in fluorescence intensity, a color scale was used.

Calibration of the Free Calcium Concentration and Fluorescence Photobleaching Recovery Analysis

An apparent free calcium concentration was calculated from the equation (calcium) = K_d [F(t) − F_{min}]/[F_{max} − F(t)], where F(t) is the fluorescence intensity of Ca-Crimson Dextran and F_{max} was measured as the fluorescence intensity after addition of ionomycin (~1 μM) in the presence of 1.5 mM extracellular calcium. F_{min} was calculated as 4% of F_{max}. The background auto fluorescence was determined by measuring the fluorescence of a cell that was not loaded with indicator and was subtracted from F, F_{min}, and F_{max}.

The diffusion analysis was performed as described in Oancea et al. (1998). In short, Gaussian photobleach bleach profiles were analyzed as a function of time to extract an apparent average diffusion coefficient and dissociation time constant.

Acknowledgments

We thank Drs. Mary Teruel and Kala Subramanian, Kang Shen, and Wen Chen for experimental support and insightful discussions during the development of the project. We would also like to thank Hiroko Yokoe for invaluable technical advice. This work was supported by the Office of Naval Research grant N000014–97–1–0911 and the National Institute of Health grant GM-51457.

Received June 23, 1998; revised September 4, 1998.

References

Abeliovich, A., Chen, C., Goda, Y., Silva, A.J., Stevens, C.F., and Tonegawa, S. (1993). Modified hippocampal long-term potentiation in PKC gamma-mutant mice. Cell *75*, 1253–1262.

Berridge, M.J. (1993). Inositol trisphosphate and calcium signaling. Nature *361*, 315–325.

Boni, L.T., and Rando, R.R. (1985). The nature of protein kinase C activation by physically defined phospholipid vesicles and diacylglycerols. J. Biol. Chem. *260*, 10819–10825.

De Koninck, P., and Schulman, H. (1998). Sensitivity of CaM kinase II to the frequency of Ca2+ oscillations. Science *279*, 227–230.

Dolmetsch, R.E., Xu, K., and Lewis, R.S. (1998). Calcium oscillations increase the efficiency and specificity of gene expression. Nature *392*, 933–936.

Hajnoczky, G., Robb-Gaspers, L.D., Seitz, M.B., and Thomas, A.P. (1995). Decoding of cytosolic calcium oscillations in the mitochondria. Cell *82*, 415–424.

Hannun, Y.A., Loomis, C.R., and Bell, R.M. (1985). Activation of protein kinase C by Triton X-100 mixed micelles containing diacylglycerol and phosphatidylserine. J. Biol. Chem. *260*, 10039–10043.

Hurley, J.H., and Gobler, J.A. (1997). Protein kinase C and phospholipase C: bilayer interactions and regulation. Curr. Opin. Struct. Biol. *7*, 557–565.

Kontos, C.D., Stauffer, T.P., Yang, W.P., Huang, L., Blanar, M.A., Meyer, T., and Peters, K.G. (1998). Activation of phosphatidilinositol 3-kinase and Aky by Tie2: a potential role for Tie2 in endotelial cell survival. Mol. Cell Biol., in press.

Li, W.-H., Llopis, J., Whitney, M., Zlokarnik, G., Tsien, R.Y. (1998). Cell permeant caged InsP3 ester shows that Ca2+ spike frequency can optimize gene expression. Nature *392*, 936–941.

Meyer, T., and Stryer, L. (1991). Calcium spiking. Annu. Rev. Biophys. Biophys. Chem. *20*, 153–174.

Meyer, T., Hanson, P.I., Stryer, L., and Schulman, H. (1992). Calmodulin trapping by calcium-calmodulin-dependent protein kinase. Science *256*, 1199–1202.

Miyawaki, A., Llopis, J., Heim, R., McCaffery, J.M., Adams, J.A., Ikura, M., and Tsien, R.Y. (1997). Fluorescent indicators for Ca2+ based on green fluorescent proteins and calmodulin. Nature *388*, 882–887.

Mochly-Rosen, D. (1995). Localization of protein kinases by anchoring proteins: a theme in signal transduction. Science *268*, 247–251.

Mosior, M., and McLaughlin, S. (1991). Peptides that mimic the pseudosubstrate region of protein kinase C bind to acidic lipids in membranes. Biophys. J. *60*, 149–159.

Mosior, M., and Newton, A.C. (1996). Calcium-independent binding to interfacial phorbol esters causes protein kinase C to associate with membranes in the absence of acidic lipids. Biochemistry *35*, 1612–1623.

Newton, A.C. (1995). Protein kinase C. Seeing two domains. Curr. Biol. *5*, 973–976.

Nishizuka, Y. (1988). The molecular heterogeneity of protein kinase C and its implications for cellular regulation. Nature *334*, 661–665.

Nishizuka, Y. (1992). Intracellular signaling by hydrolysis of phospholipids and activation of protein kinase C. Science *258*, 607–614.

Oancea, E., Teruel, M.N., Quest, A.F.G., and Meyer, T. (1998). Green fluorescent protein (GFP)-tagged cysteine-rich domains from protein kinase C as fluorescent indicators for diacylglycerol signaling in living cells. J. Cell Biol. *140*, 485–498.

Pears, C.J., and Parker, P.J. (1991). Domain interactions in protein kinase C. J. Cell. Sci. *100*, 683–686.

Quest, A.F. (1996). Regulation of protein kinase C: a tale of lipids and proteins. Enzyme Protein. *49*, 231–61.

Romoser, V.A., Hinkle, P.M., and Persechini, A. (1997). Detection in living cells of Ca2+-dependent changes in the fluorescence emission of an indicator composed of two green fluorescent protein variants linked by a calmodulin-binding sequence. A new class of fluorescent indicators. J. Biol. Chem. *272*, 13270–13274.

Sakai, N., Sasaki, K., Ikegaki,N., Shirai, Y., Ono, Y., and Saito, N. (1997). Direct visualization of the translocation of the gamma-subspecies of protein kinase C in living cells using fusion proteins with green fluorescent protein. J. Cell Biol. *139*, 1465–1476.

Schneider, H., Cohen-Dayag, A., and Pecht, I. (1992). Tyrosine phosphorylation of phospholipase C gamma 1 couples the Fc epsilon receptor mediated signal to mast cells secretion. Int. Immunol. *4*, 447–453.

Srinivasa, N., Bax, B., Blundell, T.L., and Parker, P.J. (1996). Structural aspects of the functional modules in human protein kinase-C alpha deduced from comparative analysis. Proteins *26*, 217–235.

Stauffer, T.P., and Meyer, T. (1997). Compartmentalized IgE receptor-mediated signal transduction in living cells. J. Cell Biol. *139*, 1447–1454.

Stauffer, T.P., Ahn, S., and Meyer, T. (1998). Receptor induced transient reduction in plasma membrane PtdIns(4,5)P2 concentration monitored in living cells. Curr. Biol. *8*, 343–346.

Teruel, M., and Meyer, T. (1997). Electroporation induced formation of calcium entry sites in cell body and processes of adherent cells. Biophys. J. *73*, 1785–1796.

Thomas, A.P., Bird, G.S., Hajnoczky, G., Robb-Gaspers, L.D., and Putney, J.W., Jr. (1996). Spatial and temporal aspects of cellular calcium signaling. FASEB J. *10*, 1505–1517.

Tsien, R.W., and Tsien, R.Y. (1990). Calcium channels, stores, and oscillations. Annu. Rev. Cell. Biol. *6*, 715–760.

Yokoe, H., and Meyer, T. (1996). Spatial dynamics of GFP-tagged proteins investigated by local fluorescence enhancement. Nat. Biotechnol. *14*, 1252–1256.